World Academy of Science, Engineering and Technology
International Journal of Geological and Environmental Engineering
Vol:9, No:9, 2015

Nonlinear Response of Infinite Beams on a Multilayer Tensionless Extensible Geo-Synthetic: Reinforced Earth Beds under Moving Load

K. Karuppasamy

Open Science Index, Geological and Environmental Engineering Vol:9, No:9, 2015 publications.waset.org/10002172/pdf

Abstract**—**In this paper, analysis of an infinite beam resting on multilayer tensionless extensible geosynthetic reinforced granular fill-poor soil system overlying soft soil strata under moving load with constant velocity is presented. The beam is subjected to a concentrated load moving with constant velocity. The upper reinforced granular bed is modeled by a rough membrane embedded in Pasternak shear layer overlying a series of compressible nonlinear winkler springs representing the underlying the very poor soil. The multilayer tensionless extensible geosynthetic layer has been assumed to deform such that at interface the geosynthetic and the soil have some deformation. Nonlinear behaviour of granular fill and the very poor soil has been considered in the analysis by means of hyperbolic constitutive relationships. Governing differential equations of the soil foundation system have been obtained and solved with the help of appropriate boundary conditions. The solution has been obtained by employing finite difference method by means of Gauss-Siedal iterative scheme. Detailed parametric study has been conducted to study the influence of various parameters on the response of soil–foundation system under consideration by means of deflection and bending moment in the beam and tension mobilized in the geosynthetic layer. These parameters include magnitude of applied load, velocity of load, damping, ultimate resistance of poor soil and granular fill layer. Range of values of parameters has been considered as per Indian Railway conditions. This study clearly observed that the comparisons of multilayer tensionless extensible geosynthetic reinforcement with poor foundation soil and magnitude of applied load, relative compressibility of granular fill and ultimate resistance of poor soil has significant influence on the response of soil–foundation system.

Keywords**—**Infinite beams, multilayer tensionless extensible geosynthetic, granular layer, moving load, nonlinear behavior of poor soil.

I. Introduction

REINFORCED earth is widely in use as the construction material in formation of subgrade for roads, railway tracks and in air strips to reduce the settlement and to increase the bearing capacity. Especially geotechnical engineers face several challenges in the construction of earth structures like retaining walls and embankments which cater to the development of transport infrastructure. Soil reinforcement plays a major part in strengthening of earth structures and utilization of soft foundation soils especially geotechnical engineers face several challenges in the construction of earth structures like retaining walls and embankments which cater to the development of transport infrastructure. Soil reinforcement plays a major part in strengthening of earth structures and utilization of soft foundation soils. Hence the need to develop new analytical methods for nonlinear response of multilayer tensionless extensible geosynthetic - reinforced foundation subjected to moving load under the very poor soil.

In the present work, modeling and analysis of an infinite beam resting on multilayer tensionless extensible geosynthetic reinforced-granular bed on soft soils has been studied with the lifting up partially and losing contact with the soils. The reinforcement has been considered multilayer tensionless extensible and compatibility conditions as suggested by [1], [4]-[8], [10]-[20] have been incorporated, reducing the number of parameters involved in this analysis. The foundation assumed to react only in compression. The nonlinear responses of multilayer tensionless extensible geosynthetic - reinforced foundation and foundation reaction in tension have been compared and further various parametric studies has been conducted considering values of input parameters reverent to the Indian railway conditions and the influence of various parameters of soil–foundation system. Finite difference method is used for the solution of governing differential equations of the model and all the results have been presented in non-dimensional forms. The properties of different layers of base, sub-base and foundation may be incorporated in the model by taking the equivalent stiffness of the nonlinear spring.

II. Statement of the Problem and Proposed Model

Fig. 1 shows the definition sketch of the problem considered in the infinite beam resting on multilayer tensionless extensible geosynthetic reinforced granular fill – poor soil system. The infinite beam has been founded on a granular fill layer overlying poor foundation soil of thickness (H) and subjected to concentrated moving load (P). A three geosynthetic layers have been placed inside the granular fill layer which divides the granular fill layer into four, having thicknesses as H_1, H_2, H_3 and H_4 as shown in Fig. 1. The shear modulus of four layer of granular fill are G_1, G_2, G_3, and G_4 respectively while μ_1 and μ_2 are the interface coefficients at the top and bottom faces of the top geosynthetic layer respectively; μ_2 and μ_3 are the interface coefficients at the top and bottom faces of the middle geosynthetic layer respectively; μ_3 and μ_4 are the interface coefficients at the top

K. Karuppasamy is with the Engineer III (Geotechnical Services), AECOM India Pvt. Ltd., DLF Cyber City, DLF Phase II, Gurgaon, Haryana, 122002, India. (phone: +91124 4871625; fax: +91124 483010; e-mail: Karuppasamy.K@aecom.com).

Open Science Index, Geological and Environmental Engineering Vol:9, No:9, 2015 publications.waset.org/10002172/pdf

and bottom faces of the bottom geosynthetic layer respectively. The geosynthetic reinforcement is assumed to be inextensible with stiffness greater than or equal to 4000 kN/m; as beyond this value the stiffness of the reinforcement has no effect on the settlement response. The creep effect of the geosynthetic is neglected in the analysis. The response of the beam under the action is to be found out.

Fig. 2 depicts the proposed model for the soil – foundation model under consideration. The poor soil subgrade has been idealized as nonlinear Winkler springs and the granular fill layer as Pasternak Shear layer. The granular fill layer has been assumed to be incompressible and the beam has been assumed to have a perfect contact with granular fill layer. A rough elastic membrane has been used to model the geosynthetic layer. A hyperbolic nonlinear stress- displacement relationship proposed by [9] has been considered to exhibit the behaviour of granular fill and poor foundation soil.

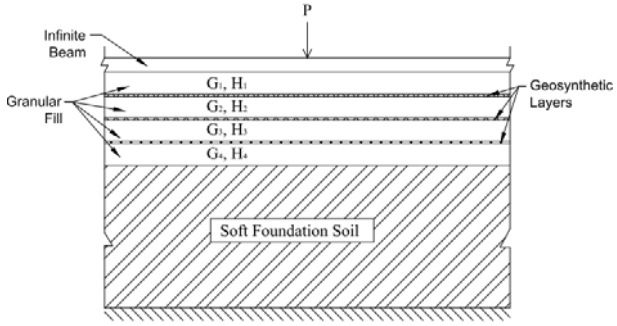


Fig. 1 Definition sketch of multilayer geosynthetic- reinforced granular fill soft soil system

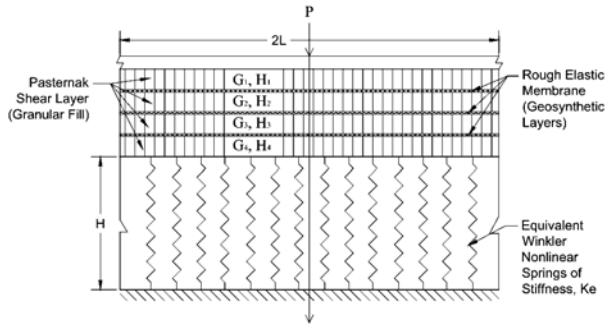


Fig. 2 Definition sketch of proposed model for soil foundation system

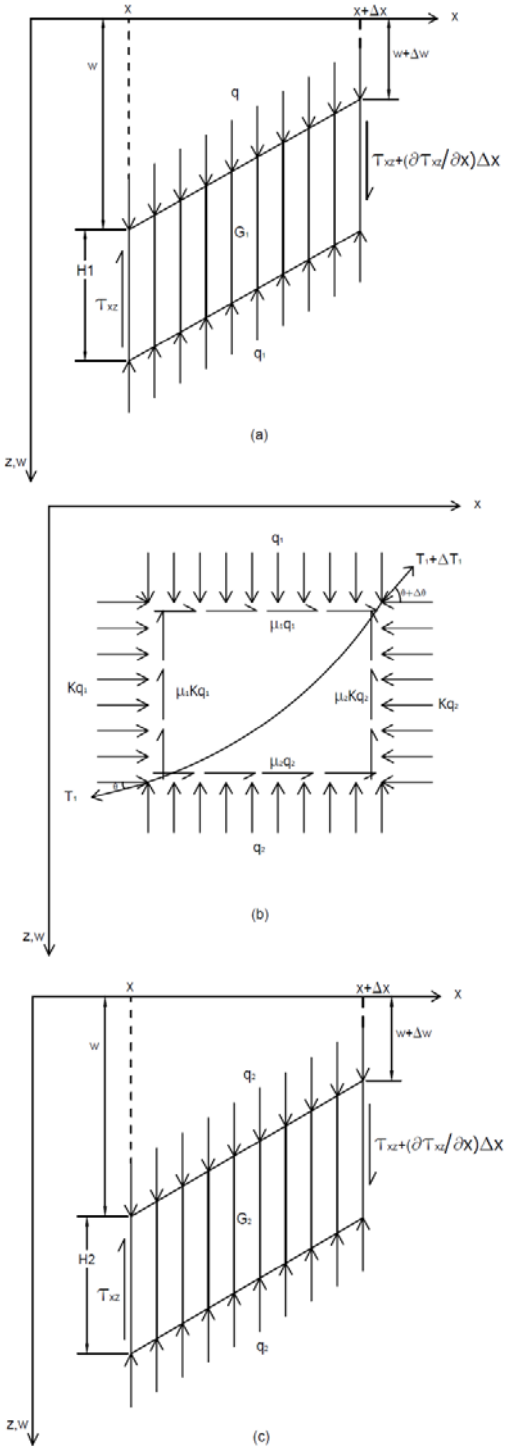
III. Analysis

Fig. 3 presents the free body diagram of the first shear layer, the rough elastic membrane element on first geosynthetic layer, the second shear layer, the rough elastic membrane element on second geosynthetic layer, the third shear layer, the rough elastic membrane element on third geosynthetic layer and fourth shear layer elements.

The vertical force equilibrium equation of the first shear layer element (Fig. 3 (a)) can be written as;

$$q = q_1 - G_1 H_1 \frac{\partial^2 w(x,t)}{\partial x^2} \quad (1)$$

where, q is the reaction of granular fill on the beam. q_1 is the vertical force interaction between the membrane and the first shear layer, w (x, t) is the vertical surface deflection, G_1 is the shear modulus first shear layer, H_1 is the thickness of the first shear layer, x is the horizontal space coordinate measured along the length of the beam and t is any particular instant of time.



Open Science Index, Geological and Environmental Engineering Vol:9, No:9, 2015 publications.waset.org/10002172/pdf

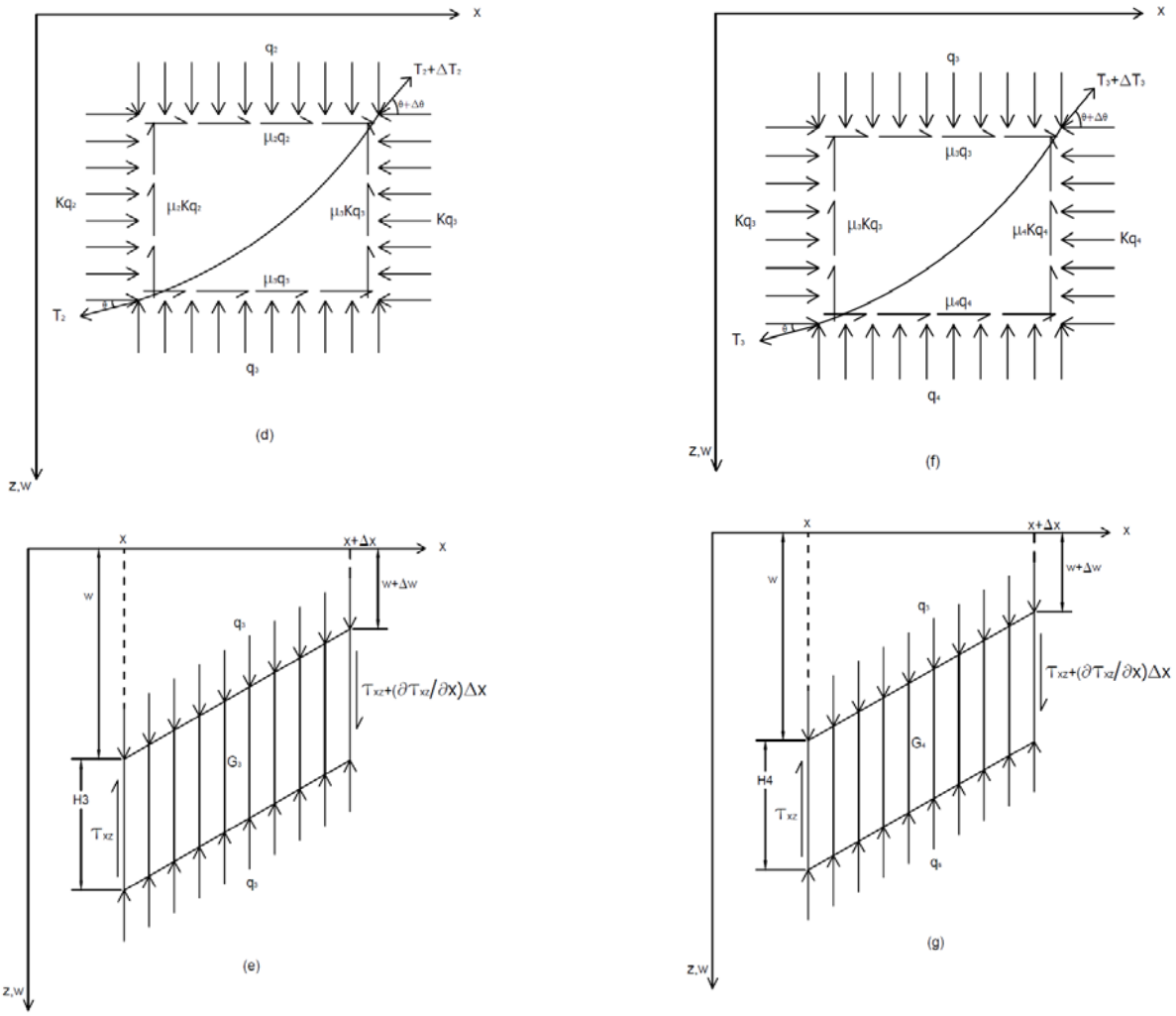


Fig. 3 Definition (a) forces on first shear layer; (b) forces on stretched rough elastic membrane element on first geosynthetic layer; (c) forces on second shear layer; (d) forces on stretched rough elastic membrane element on second geosynthetic layer; (e) forces on third shear layer; (f) forces on stretched rough elastic membrane element on third geosynthetic layer; (g) forces on fourth shear layer

The horizontal / vertical force equilibrium equation of the top rough elastic membrane element (Refer to Fig. 3 (b)) at time t > o, can be written as;

$$\cos\theta\frac{\partial T_1(x,t)}{\partial x}-T_1\sin\theta\frac{\partial\theta}{\partial x}=-(\mu_1 q_1+\mu_2 q_2)-K(q_1-q_2)\tan\theta \quad (2)$$

$$\sin\theta\frac{\partial T_1(x,t)}{\partial x}+T_1\cos\theta\frac{\partial\theta}{\partial x}=-K(\mu_1 q_1+\mu_2 q_2)\tan\theta+(q_1-q_2) \quad (3)$$

where, q_1 andq_2 are the vertical force interaction between the membrane, and the first and second shear layer respectively; $\mu_1$and μ_2 are the interface coefficients at the top and middle faces of membrane respectively, K is the coefficient of lateral stress, θ is the slope of the membrane, $T_1(x, t)$ is the tensile force per unit length mobilized in the top face of membrane.

The vertical force equilibrium equation of the second shear layer element (Fig. 3 (c)) can be written as;

$$q_2=q_2-G_2H_2\frac{\partial^2 w(x,t)}{\partial x^2} \quad (4)$$

where, q_2 is the vertical force interaction between the second shear layer and the poor foundation G_2H_2 soil, and are the shear modulus and thickness of the second shear layer respectively.

The horizontal / vertical force equilibrium equation of the middle rough elastic membrane element (Fig. 3 (d)) at time t > o, can be written as;

$$\cos\theta\frac{\partial T_2(x,t)}{\partial x}-T_2\sin\theta\frac{\partial\theta}{\partial x}=-(\mu_2 q_2+\mu_3 q_3)-K(q_2-q_3)\tan\theta \quad (5)$$

$$\sin\theta\frac{\partial T_2(x,t)}{\partial x}+T_2\cos\theta\frac{\partial\theta}{\partial x}=-K(\mu_2 q_2+\mu_3 q_3)\tan\theta+(q_2-q_3) \quad (6)$$

where, q_2 and q_3 are the vertical force interaction between the membrane and the second and third shear layer respectively; μ_2 and μ_3 are the interface coefficients at the middle and bottom faces of membrane respectively, $T_2(x, t)$ is the tensile force per unit length mobilized in the middle face of membrane.

The vertical force equilibrium equation of the third shear

Open Science Index, Geological and Environmental Engineering Vol:9, No:9, 2015 publications.waset.org/10002172/pdf

layer element (Fig. 3 (e)) can be written as;

$$q_3 = q_3 - G_3 H_3 \frac{\partial^2 w(x,t)}{\partial x^2} \tag{7}$$

where, q_3 is the vertical force interaction between the third shear layer and the poor foundation G_3H_3 soil, and are the shear modulus and thickness of the third shear layer respectively.

The horizontal / vertical force equilibrium equation of the bottom rough elastic membrane element (Fig. 3 (f)) at time t > o, can be written as;

$$\cos\theta \frac{\partial T_3(x,t)}{\partial x} - T_3 \sin\theta \frac{\partial \theta}{\partial x} = -(\mu_3 q_3 + \mu_4 q_4) - K(q_3 - q_4)\tan\theta \tag{8}$$

$$\sin\theta \frac{\partial T_3(x,t)}{\partial x} + T_3 \cos\theta \frac{\partial \theta}{\partial x} = -K(\mu_3 q_3 + \mu_4 q_4)\tan\theta + (q_3 - q_4) \tag{9}$$

where, q_3 and q_4 are the vertical force interaction between the membrane and the third and fourth shear layer respectively; μ_3 and μ_4 are the interface coefficients at the bottom faces of membrane, $T_3(x, t)$ is the tensile force per unit length mobilized in the bottom face of membrane.

The vertical force equilibrium equation of the fourth shear layer element (Fig. 3 (g)) can be written as;

$$q_4 = q_s - G_4 H_4 \frac{\partial^2 w(x,t)}{\partial x^2} \tag{10}$$

where, q_s is the vertical force interaction between the fourth layer of granular fill G_4H_4 and the poor foundation soil, and are the shear modulus and thickness of the fourth layer of granular fill respectively from (4) and (5), one can write,

$$q_1 = q_2 + \frac{T_1 \sec\theta}{(1 + K\tan^2\theta)} \frac{\partial \theta}{\partial x} - \frac{(1-K)(\mu_1 q_1 + \mu_2 q_2)\tan\theta}{(1 + K\tan^2\theta)} \tag{11}$$

Substituting for $\frac{\partial \theta}{\partial x}$ in terms of vertical displacement, w(x, t) in to (13), and one can write;

$$q_1 = \bar{X}_1 q_2 - \bar{X}_2 T_1 \cos\theta \frac{\partial^2 w(x,t)}{\partial x^2} \tag{12}$$

Similarly; from (7) and (8), we get,

$$q_2 = \bar{X}_3 q_3 - \bar{X}_4 T_2 \cos\theta \frac{\partial^2 w(x,t)}{\partial x^2} \tag{13}$$

From (10) and (11), we get

$$q_3 = \bar{X}_5 q_4 - \bar{X}_6 T_3 \cos\theta \frac{\partial^2 w(x,t)}{\partial x^2} \tag{14}$$

where,

$$\bar{X}_1 = \frac{1 + K\tan^2\theta - (1-K)\mu_2 \tan\theta}{1 + K\tan^2\theta + (1-K)\mu_1 \tan\theta} \tag{15a}$$

$$\bar{X}_3 = \frac{1 + K\tan^2\theta - (1-K)\mu_3 \tan\theta}{1 + K\tan^2\theta + (1-K)\mu_2 \tan\theta} \tag{15b}$$

$$\bar{X}_4 = \frac{1}{1 + K\tan^2\theta + (1-K)\mu_2 \tan\theta} \tag{15c}$$

$$\bar{X}_5 = \frac{1 + K\tan^2\theta - (1-K)\mu_4 \tan\theta}{1 + K\tan^2\theta + (1-K)\mu_3 \tan\theta} \tag{15d}$$

$$\bar{X}_6 = \frac{1}{1 + K\tan^2\theta + (1-K)\mu_3 \tan\theta} \tag{15e}$$

Combining (1), (4), (7), (10), (12), (13) and (14)

$$q = q_s \bar{X}_1 \bar{X}_3 \bar{X}_5 - (G_1 H_1 + G_2 H_2 \bar{X}_1 + G_3 H_3 \bar{X}_1 \bar{X}_3 + G_4 H_4 \bar{X}_1 \bar{X}_3 \bar{X}_5 + \bar{X}_2 T_1 \cos\theta + \bar{X}_1 \bar{X}_4 T_2 \cos\theta + \bar{X}_1 \bar{X}_3 \bar{X}_6 T_3 \cos\theta) \frac{\partial^2 w(x,t)}{\partial x^2} \tag{16}$$

From (4), (5), (7), (8), (10), and (11), we get

$$\frac{\partial T_1(x,t)}{\partial x} = (q_1 - q_2)(1-K)\sin\theta - (\mu_1 q_1 + \mu_2 q_2)(1 + K\tan^2\theta)\cos\theta \tag{17}$$

$$\frac{\partial T_1(x,t)}{\partial x} = -q_1 \bar{Y}_1 - q_2 \bar{Y}_2 \tag{18}$$

$$\frac{\partial T_2(x,t)}{\partial x} = -q_2 \bar{Y}_3 - q_3 \bar{Y}_4 \tag{19}$$

$$\frac{\partial T_3(x,t)}{\partial x} = -q_3 \bar{Y}_5 - q_4 \bar{Y}_6 \tag{20}$$

Combining (1), (4), (7), (10) and (11) following equation can be obtained:

$$\frac{\partial T_1(x,t)}{\partial x} = -\bar{Y}_1 \left(q + G_1 H_1 \frac{\partial^2 w(x,t)}{\partial x^2} \right) - \bar{Y}_2 \left(\overline{X_3 X_5} q_s - \left(G_2 H_2 + \bar{X}_3 G_3 H_3 + \overline{X_3 X_5} G_4 H_4 + \bar{X}_4 T_2 \cos\theta + \overline{X_3 X_6} T_3 \cos\theta \right) \frac{\partial^2 w(x,t)}{\partial x^2} \right) \tag{21}$$

$$\frac{\partial T_2(x,t)}{\partial x} = -\bar{Y}_3 \left(\frac{1}{\bar{X}_3} \left(q + (G_1 H_1 + \bar{X}_2 T_1 \cos\theta) \frac{\partial^2 w(x,t)}{\partial x^2} \right) + G_2 H_2 \frac{\partial^2 w(x,t)}{\partial x^2} \right) - \bar{Y}_4 \left(\bar{X}_5 q_s - \left(G_3 H_3 + \bar{X}_5 G_4 H_4 + \bar{X}_6 T_3 \cos\theta \right) \frac{\partial^2 w(x,t)}{\partial x^2} \right) \tag{22}$$

$$\frac{\partial T_3(x,t)}{\partial x} = -\frac{\bar{Y}_5}{\overline{X_1 X_3}} \left(q + (G_1 H_1 + \bar{X}_1 G_2 H_2 + \overline{X_1 X_3} G_3 H_3 + \bar{X}_2 T_1 \cos\theta + \overline{X_1 X_4} T_2 \cos\theta) \frac{\partial^2 w(x,t)}{\partial x^2} \right) - \bar{Y}_6 (q_s - G_4 H_4) \frac{\partial^2 w(x,t)}{\partial x^2} \tag{23}$$

where,

$$\bar{Y}_1 = (\mu_1 \cos\theta (1 + K\tan^2\theta) - (1-K)\sin\theta) \tag{24a}$$

$$\bar{Y}_2 = (\mu_2 \cos\theta (1 + K\tan^2\theta) + (1-K)\sin\theta) \tag{24b}$$

$$\bar{Y}_3 = (\mu_2 \cos\theta (1 + K\tan^2\theta) - (1-K)\sin\theta) \tag{24c}$$

$$\overline{Y_4} = (\mu_3 \cos\theta(1 + K\tan^2\theta) + (1-K)\sin\theta) \quad (24d)$$

$$\overline{Y_5} = (\mu_3 \cos\theta(1 + K\tan^2\theta) - (1-K)\sin\theta) \quad (24e)$$

$$\overline{Y_6} = (\mu_4 \cos\theta(1 + K\tan^2\theta) + (1-K)\sin\theta) \quad (24f)$$

Considering the hyperbolic shear stress – shear strain response of the granular fill proposed by [3]; the shear modulus of different granular layers (G_1, G_2, G_3 and G_4) can be expressed as;

$$G_j = \frac{G_{j0}}{\left[1 + \frac{G_{j0}|dw/dx|}{\tau_{uj}}\right]^2} \quad (25)$$

where, G_{jo} is initial shear modulus of granular layer 1, 2, 3 and 4 respectively; τ_{uj} is the ultimate shear resistance of the granular layer 1, 2, 3 and 4 respectively; dw/dx is the shear strain.

Considering the hyperbolic nonlinear Stress- displacement relationship [9], q_s can be expressed as,

$$q_s = \frac{k_{s0} w}{1 + \frac{k_{s0} w}{q_u}} \quad (26)$$

where, k_{so} is the initial modulus of subgrade reaction of poor soil and q_u is the ultimate bearing capacity of the poor soil.

The differential equation of a moving load on the beam may be obtained by considering the bending of an elemental segment. The differential equation of the beam with uniform cross section can be written as:

$$EI\frac{d^4w}{dx^4} + \rho\frac{d^2w}{dt^2} + c\frac{dw}{dt} + q = P(x,t) \quad (27)$$

where, w(x, t) is the deflection of the beam, EI is the flexural rigidity of the beam, ρ is the mass per unit length of the beam, c is the coefficient of viscous damping per unit length of the beam, P(x, t) is the applied load intensity, In the absence of damping (14) can be written as,

$$EI\frac{d^4w}{dx^4} + \rho\frac{d^2w}{dt^2} + q = P(x,t) \quad (28)$$

Equations (16), (21), (22) and (23) govern of the response of the proposal model in the absence of damping. For particular values of the parameters, these equations govern the response of existing models for beams on elastic foundation subjected to moving load [2].

IV. Solution of the Governing Equations

The response of system has been represented as a function of distance (x) from the center of the beam at time (t). For simplicity, substituting $\xi = x - vt$ where,' ξ' is the distance from the point of action of loading at time 't'. The governing differential equations have only one variable ξ.

From (16), (21), (22) and (23) can be written as;

$$q = q_s\overline{X}_1\overline{X}_3\overline{X}_5 - (G_1H_1 + G_2H_2\overline{X}_1 + G_3H_3\overline{X}_1\overline{X}_3 + G_4H_4\overline{X}_1\overline{X}_3\overline{X}_5 + \overline{X}_2T_1\cos\theta + \overline{X}_1\overline{X}_4T_2\cos\theta + \overline{X}_1\overline{X}_3\overline{X}_6T_3\cos\theta)\frac{\partial^2 w}{\partial\xi^2} \quad (29)$$

$$\frac{\partial T_1}{\partial\xi} = -\overline{Y_1}\left(q + G_1H_1\frac{\partial^2 w}{\partial\xi^2}\right) - \overline{Y_2}\left(\overline{X_3}\,\overline{X_5}q_s - \left(G_2H_2 + \overline{X_3}G_3H_3 + \overline{X_3}\,\overline{X_5}G_4H_4 + \overline{X_4}T_2\cos\theta + \overline{X_3}\,\overline{X_6}T_3\cos\theta\right)\frac{\partial^2 w}{\partial\xi^2}\right) \quad (30)$$

$$\frac{\partial T_2}{\partial\xi} = -\overline{Y_3}\left(\frac{1}{\overline{X_3}}\left(q + (G_1H_1 + \overline{X_2}T_1\cos\theta)\frac{\partial^2 w}{\partial\xi^2}\right) + G_2H_2\frac{\partial^2 w}{\partial\xi^2}\right) - \overline{Y_4}\left(\overline{X_5}q_s - \left(G_3H_3 + \overline{X_5}G_4H_4 + \overline{X_6}T_3\cos\theta\right)\frac{\partial^2 w}{\partial\xi^2}\right) \quad (31)$$

$$\frac{\partial T_3}{\partial\xi} = -\frac{\overline{Y_5}}{\overline{X_1}\,\overline{X_3}}\left(q + \left(G_1H_1 + \overline{X_1}G_2H_2 + \overline{X_1}\,\overline{X_3}G_3H_3 + \overline{X_2}T_1\cos\theta + \overline{X_1}\,\overline{X_4}T_2\cos\theta\right)\frac{\partial^2 w}{\partial\xi^2}\right) - \overline{Y_6}\left(q_s - G_4H_4\right)\frac{\partial^2 w}{\partial\xi^2}\right) \quad (32)$$

$$EI\frac{d^4w}{d\xi^4} + \rho v^2\frac{d^2w}{d\xi^2} + q = P(\xi) \quad (33)$$

To observe the settlement response of the proposed model, (29)-(33) have been written in non-dimensional of finite difference from within the specified space domain for an interior node i, one obtains;

$$q_i^* = A_1W_i\overline{X}_1\overline{X}_3\overline{X}_5 - (G_1^* + G_2^*\overline{X}_1 + G_3^*\overline{X}_1\overline{X}_3 + G_4^*\overline{X}_1\overline{X}_3\overline{X}_5 + \overline{X}_2T_{1i}^*\cos\theta + \overline{X}_1\overline{X}_4T_{2i}^*\cos\theta + \overline{X}_1\overline{X}_3\overline{X}_6T_{3i}^*\cos\theta)\frac{\partial^2 W}{\partial\xi^{*2}} \quad (34)$$

$$T_{1(i+1)}^* = T_{1i}^* - \overline{Y_1}\Delta\xi^*\left(q_i^* + G_1^*\frac{\partial^2 W}{\partial\xi^{*2}}\right) - \overline{Y_2}\Delta\xi^*\left(\overline{X_3}\,\overline{X_5}A_1W_i - \left(G_2^* + \overline{X_3}G_3^* + \overline{X_3}\,\overline{X_5}G_4^* + \overline{X_4}T_{2i}^*\cos\theta + \overline{X_3}\,\overline{X_6}T_{3i}^*\cos\theta\right)\frac{\partial^2 W}{\partial\xi^{*2}}\right) \quad (35)$$

$$T_{2(i+1)}^* = T_{2i}^* - \overline{Y_3}\Delta\xi^*\left(\frac{1}{\overline{X_3}}\left(q_i^* + (G_1^* + \overline{X_2}T_{1i}^*\cos\theta)\frac{\partial^2 W}{\partial\xi^{*2}}\right) + G_2^*\frac{\partial^2 W}{\partial\xi^{*2}}\right) - \overline{Y_4}\Delta\xi^*\left(\overline{X_5}A_1W_i - \left(G_3^* + \overline{X_5}G_4^* + \overline{X_6}T_{3i}^*\cos\theta\right)\frac{\partial^2 W}{\partial\xi^{*2}}\right) \quad (36)$$

$$T_{3(i+1)}^* = T_{3i}^* - \frac{\overline{Y_5}}{\overline{X_1}\,\overline{X_3}}\Delta\xi^*\left(q_i^* + \left(G_1^* + \overline{X_1}G_2^* + \overline{X_1}\,\overline{X_3}G_3^* + \overline{X_2}T_{1i}^*\cos\theta + \overline{X_1}\,\overline{X_4}T_{2i}^*\cos\theta\right)\frac{\partial^2 W}{\partial\xi^{*2}}\right) - \overline{Y_6}\Delta\xi^*\left(A_1W_i - G_4^*\right)\frac{\partial^2 W}{\partial\xi^{*2}}\right) \quad (37)$$

Open Science Index, Geological and Environmental Engineering Vol:9, No:9, 2015 publications.waset.org/10002172/pdf

$$W_i = \frac{1}{\left(6 - 2\frac{\rho^* \times \Delta\xi^{*2}}{I^*}\right)} \times \left[\frac{P^* \Delta\xi^{*3}}{I^*} - \frac{q_i^* \times \Delta\xi^{*4}}{I^*} - W_{i-2} - W_{i+2} - \left(-4 + \frac{\rho^* \times \Delta\xi^{*2}}{I^*}\right) \times W_{i-1} - \left(-4 + \frac{\rho^* \times \Delta\xi^{*2}}{I^*}\right) \times W_{i+1}\right] \quad (38)$$

where; $P^* = P / k_{s0} L^2 d\xi^*$; $G_1^* = G_1 H_1 / k_{s0} L^2$; $G_4^* = G_4 H_4 / k_{s0} L^2$; $G_2^* = G_2 H_2 / k_{s0} L^2$; $\xi^* = \xi / L$; $\tau_{u2}^* = \tau_{u2} / k_{s0} L$; $G_3^* = G_3 H_3 / k_{s0} L^2$ $W = w / L$; $\tau_{u1}^* = \tau_{u1} / k_{s0} L$; $\tau_{u3}^* = \tau_{u3} / k_{s0} L$; $\tau_{u4}^* = \tau_{u4} / k_{s0} L$; $q^* = q / k_{s0} L$; $I^* = EI / k_{s0} L^4$; $q_u^* = q_u / k_{s0} L$; $\rho^* = \rho v^2 / k_{s0} L^2$; $T_1^* = T_1 / k_{s0} L^2$; $T_2^* = T_2 / k_{s0} L^2$; $T_3^* = T_3 / k_{s0} L^2$ and P is the applied load, and L is half the length of the beam considered.

Finite difference formulation has been employed to solve the differential equations. In these equations, the derivatives are expressed by central difference method as follows;

$$\frac{d^4 W}{d\xi^{*4}} = \left(\frac{W_{i-2} - 4W_{i-1} + 6W_i - 4W_{i+1} + W_{i+2}}{\Delta\xi^{*4}}\right) \quad (39a)$$

$$\frac{d^2 W}{d\xi^{*2}} = \left(\frac{W_{i-1} - 2W_i + W_{i+1}}{(\Delta\xi^*)^2}\right) \quad (39b)$$

$$\frac{dW}{d\xi^*} = \left(\frac{W_{i+1} - W_{i-1}}{(2 * \Delta\xi^*)}\right) \quad (39c)$$

From (35) to (37) in the term $dT^* / d\xi^*$ is written in backward difference from for $-1 \le \xi^* \ge 0$, whereas for $0 \le \xi^* \ge 1$ forward difference is used for the same.

V. Boundary Conditions

Boundary conditions have been considered at the edge of the beam. At both ends of the beam, the deflection of the beam, the slope of the deflected shape of the beam and the mobilized tension are zero. These boundary conditions can be written in non-dimensional form as: at ξ^* = -1 and 1, $W = 0, \frac{dW}{d\xi^*} = 0$ and $T^* = 0$.

Since, from (34) to (38) are all nonlinear equations; an iterative computing procedure has been used for obtaining solutions. The solutions have been obtained with a convergence criterion as,

$$\left|\frac{W_i^k - W_i^{k-1}}{W_i^k}\right| < \varepsilon \quad \& \quad \left|\frac{T_i^k - T_i^{k-1}}{T_i^k}\right| < \varepsilon$$

where; i- is the no of elements; k & k-1 are the present and previous iteration values, respectively; ε is the specified tolerance limit, which is 10^{-10} in the present study.

VI. Results and Discussions

Based on the formulation presented in previous chapter, a computer program was developed using finite difference scheme. Complete region of the problem (- L≤ x ≤ L) was considered. The total length of the beam (2L) was divided into different numbers of elements and it was observed that the difference in results corresponding to 800 and 1000 numbers of elements was less than 0.5% hence 800 elements were used and the solution was obtained with a tolerance limit of 10^{-5}. Half the length of the beam is taken to be large enough for the beam to be assumed to act as an infinite beam. The following values of parameters have been adopted for the parameter study as shown in Table I.

For a typical set of parameters, i.e., P^*= 5 x 10^{-7}, $G_{to}^* = G_{bo}^*$= 3x10^{-7}, I^*=6x10^{-10}, $\tau_{ut}^* = \tau_{ub}^*$=2.7x$10^{-9}$, q_u^*=1.8x10^{-5}, ρ^*= 1.2x10^{-7}, $\mu_t = \mu_b$=0.5 and K=0.172. The comparison of nonlinear responses of the multilayer tension and multilayer tensionless extensible geosynthetic resting on nonlinearity in the behavior at poor soil which responds in infinite beam in terms of normalized deflection, normalized mobilized tension in top, middle & bottom geosynthetic layer, normalized bending moment, normalized soil reaction has been presented in Figs. 4-10. As expected, the deflection of beam has been found to increase the negative deflection of beam as the analysis considers multilayer tensionless extensible geosynthetic nonlinearity in the behavior at poor soil (Figs. 4 and 5). The maximum negative normalized deflection increase from 3.397x10^{-6} to 3.425x10^{-6}; it can be observed that the soil uniformly responding to tension under the nonlinear behavior of poor soil (Tensionless foundation) as shown in Fig. 5. So it is clear that a tensionless foundation affects the uniformly lift up of the beam (negative deflection) more as compared to its settlement (positive deflection). The comparisons are also made with respect to normalized bending moment of the beam and it is normalized mobilized tension in top, middle & bottom geosynthetic layer in Figs. 6 and 9 respectively for the same parameters as in case of deflection of beam. The maximum positive normalized bending moment is almost same for both the cases but the negative normalized bending moment decrease by around 4.6% in case of soil unable to take any tension under the nonlinear behavior of poor soil. The normalized mobilized tension is significantly affected and is negligible in case of tension foundation under the nonlinearity soil. The mobilized tension at the point of loading increases 10.8% when the soil react the tension and compression.

Figs. 10-13 show the comparison of linear and nonlinear response of the infinite beam and geosynthetic resting on poor soil which responds only in compression (Tensionless foundation) to that of soil for typical parameters, i.e., P* = 5.42 x10^{-5}, q_u^* = 5x10^{-4}, $G_{1o}^* = G_{4o}^*$ = 1.63x10^{-5}; $\tau_{u1}^* = \tau_{u4}^*$ = 1.5x10^{-4}; ρ^* = 3.12x10^{-5}; I* = 3.31x10^{-8}; $\mu_1 = \mu_4$ = 0.5; and K=0.172. As expected, the deflection of infinite beam has been found to reduce as the analysis considers non-linearity in the behavior at poor soil (Fig. 10). The maximum negative normalized deflection increase from 3.41 x 10^{-6} to 3.426 x10^{-6}; As expected, the deflection of beam has been found to almost same for the both the cases but the negative normalized deflection decrease by around 0.47% in case of soil unable to

Open Science Index, Geological and Environmental Engineering Vol:9, No:9, 2015 publications.waset.org/10002172/pdf

take any nonlinearity in the behaviour at poor foundation soil. The comparisons are also made with respect to normalized mobilized tension in multilayer extensible geosynthetic layers and they are normalized bending moment of the beam in Figs. 4 and 5 respectively for the same parameters as in case of deflection of beam. The maximum mobilized tension of multilayer extensible geosynthetic layers and normalized bending moment of the beam have been found to be almost same for both the cases for linear analysis as compared to that for nonlinear analysis.

TABLE I
RANGE OF VALUES OF VARIOUS PARAMETERS CONSIDERED FOR PARAMETRIC STUDY

Parameters	Symbol	Range of values	Unit
Applied Load	P	100 – 250	KN
Mass per unit length of beam	ρ	52	Kg/m
Flexural Rigidity of beam	EI	$4.47x10^6$ (Shahu et al.2000)	N- m^2
Modulus of sub-grade reaction for poor foundation soil	k_{so}	15 (Das, 1999)	$MN/m^2/m$
Shear modulus of granular fill	G_{1o} to G_{4o}	652.4 (Desai and Abel, 1987)	KN/m^2
Velocity of applied load	ν	40 – 140	Km/hr
Thickness of granular fill layers	H_1 to H_4	0.15	m
Ultimate bearing capacity of the poor foundation soil	q_u	20 – 60	KN/m^2
Ultimate shear resistance of granular fill	τ_{u1} to τ_{u4}	6	KN/m^2
Half-length of beam	L	150	m
Coefficient of lateral earth pressure	K	0.172	-
Interfacial friction coefficient at top and bottom reinforcement	μ_1 to μ_4	0.5	-

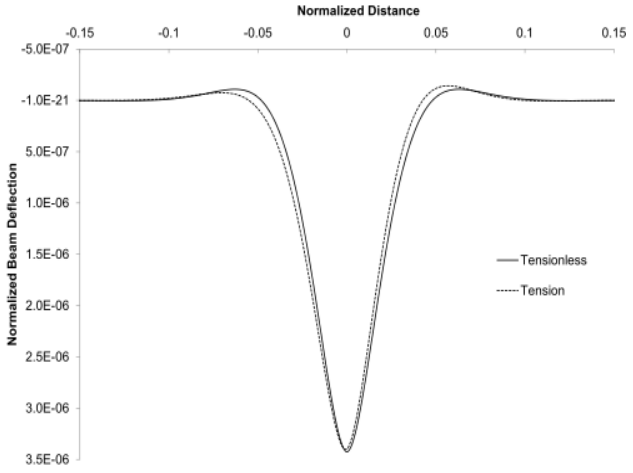


Fig. 4 Typical Settlement profiles for soil responding to tension and soil not responding to tension (i.e. Tensionless Foundation)

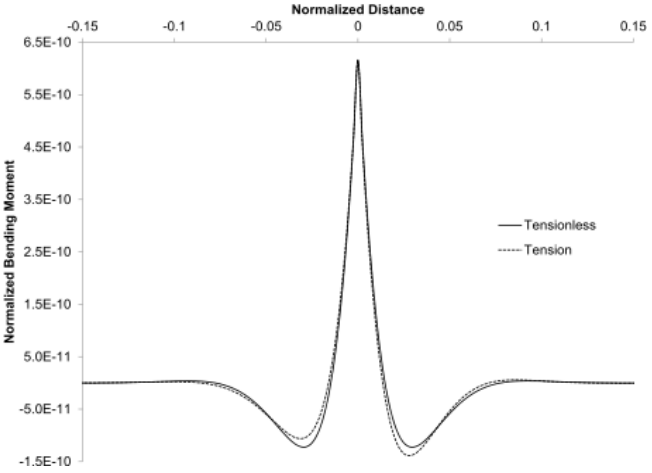


Fig. 6 Typical bending moment of beam for soil responding to tension and soil not responding to tension

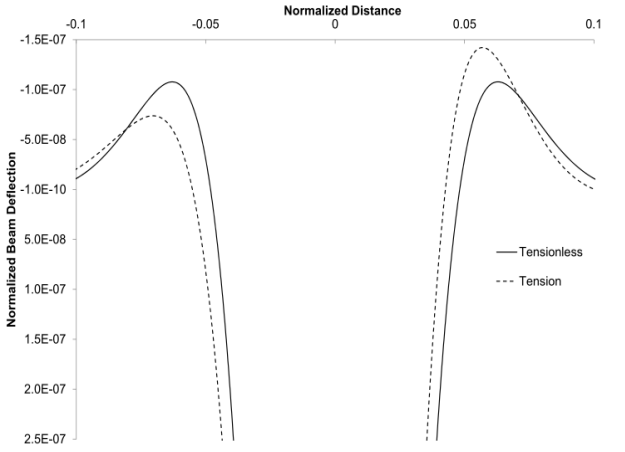


Fig. 5 Typical negative settlement profiles for soil responding to tension and soil not responding to tension

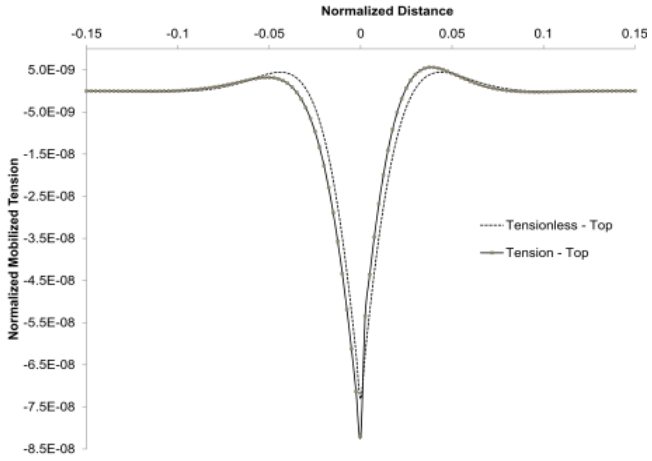


Fig. 7 Typical mobilized tension profiles of top geosynthetic layer for soil responding to tension and soil not responding to tension

Open Science Index, Geological and Environmental Engineering Vol:9, No:9, 2015 publications.waset.org/10002172/pdf

Open Science Index, Geological and Environmental Engineering Vol:9, No:9, 2015 publications.waset.org/10002172/pdf

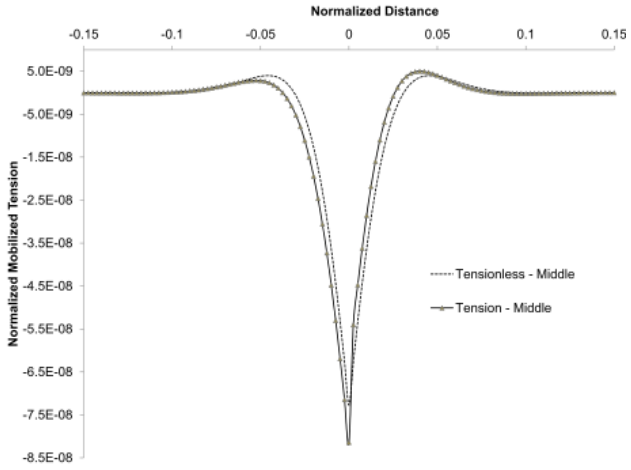


Fig. 8 Typical mobilized tension profiles of middle geosynthetic layer for soil responding to tension and soil not responding to tension

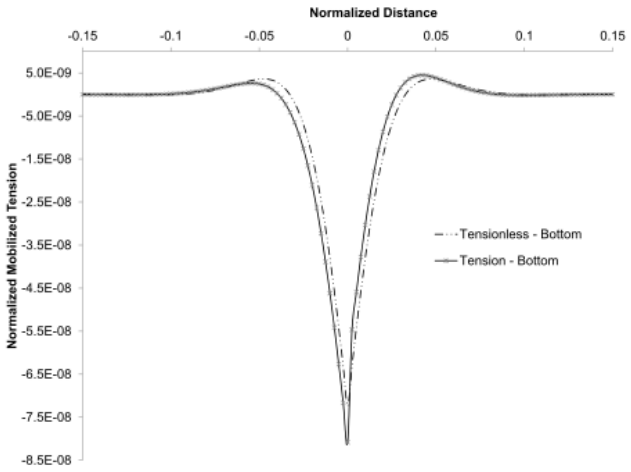


Fig. 9 Typical mobilized tension profiles of bottom geosynthetic layer for soil responding to tension and soil not responding to tension

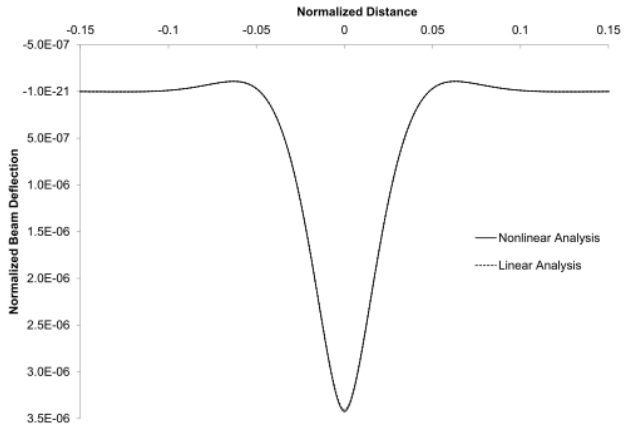


Fig. 10 Typical settlement profiles for linear and nonlinear response of multilayer tensionless extensible geosynthetic reinforced earth beds

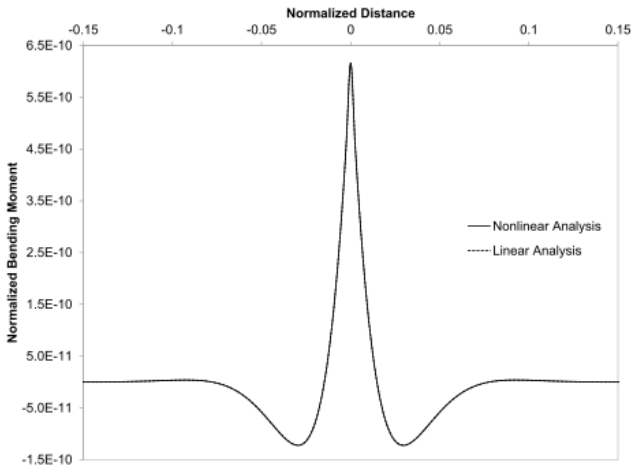


Fig. 11 Typical bending moment of beam for linear and nonlinear response of multilayer tensionless extensible geosynthetic reinforced earth beds

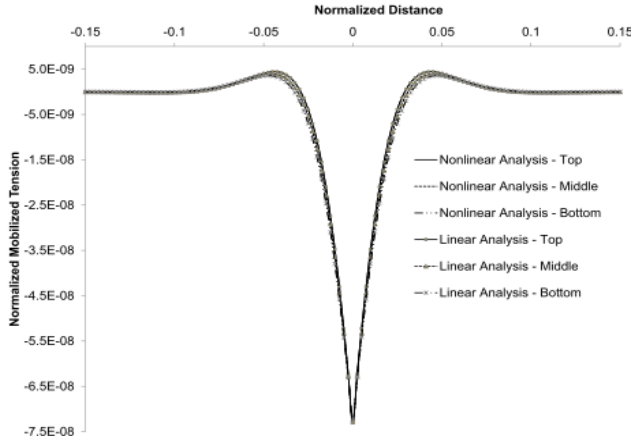


Fig. 12 Typical mobilized tension of multilayer geosynthetic layer for linear and nonlinear response of multilayer tensionless extensible geosynthetic reinforced earth beds

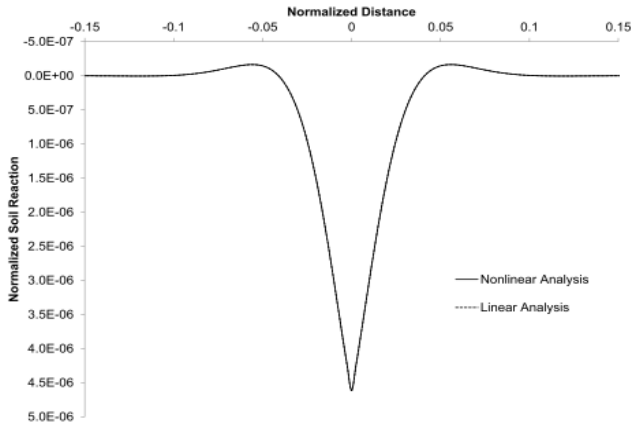


Fig. 13 Typical soil reaction profiles for linear and nonlinear response of multilayer tensionless extensible geosynthetic reinforced earth beds

The influence of ultimate resistance of poor foundation soil for multilayer extensible geosynthetic reinforced on response

Open Science Index, Geological and Environmental Engineering Vol:9, No:9, 2015 publications.waset.org/10002172/pdf

of soil- foundation system has been depicted in Figs. 14-18 for parameters, i.e., $P^*=5.42x10^{-5}$, $G_{to}{}^*=G_{4o}{}^*=1.63x10^{-5}$, K= 0.172, $I^*=3.31x10^{-8}$, $\tau_{u1}{}^*=\tau_{u4}{}^*=1.5x10^{-4}$; $\mu_1=\mu_4=0.5$; and $\rho^*=3.12x10^{-5}$. It can be observed that ultimate resistance of poor foundation soil significantly affect the response of system under consideration. The maximum normalized deflection has been found to reduce by 56% (Fig. 14) as the normalized ultimate resistance of poor foundation soil increase from $2.0x10^4$ to $6.0x10^4$. Figs. 15-17 show the effect of parameter q_u on normalized mobilized tension in top, middle & bottom of tensionless extensible geosynthetic layers. As expected, the mobilized tension in multilayer tensionless extensible geosynthetic layers have been found to reduce with an increase in the parameter, q_u. A reduction of about 67.3% in tension mobilized in multilayer tensionless extensible geosynthetic layers have been observed for various ultimate resistance of poor soil. The corresponding reduction in maximum normalized bending moment has been found to be about 77 % (Fig. 18).

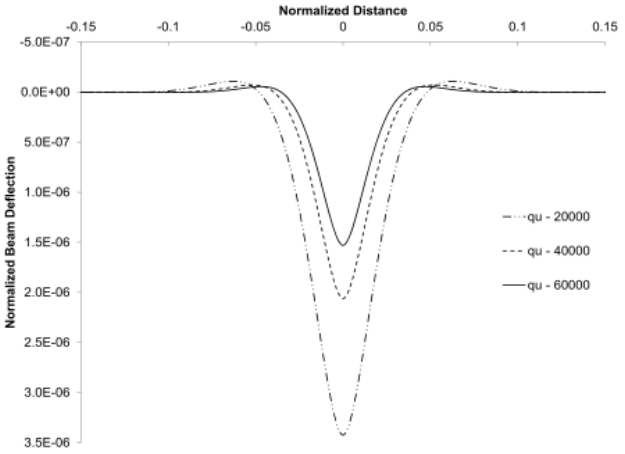


Fig. 14 Typical settlement profiles for various soil reactions

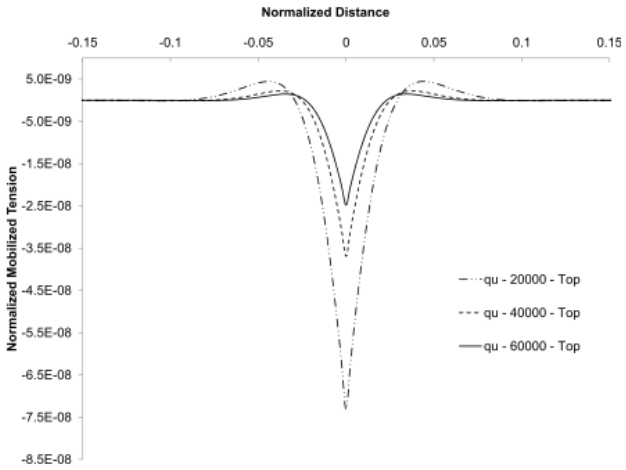


Fig. 15 Typical mobilized tension of top geosynthetic layer for various soil reactions

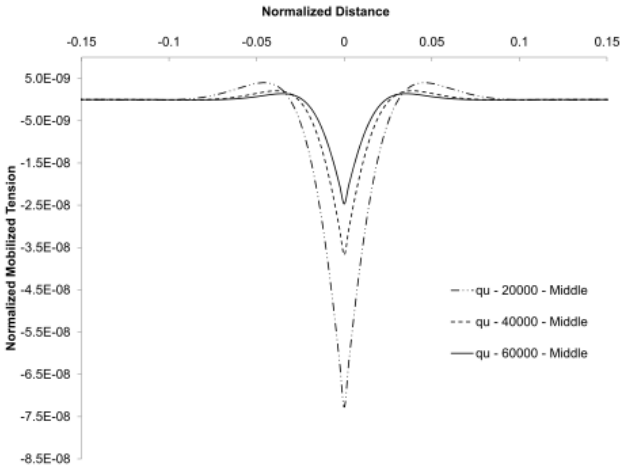


Fig. 16 Typical mobilized tension of middle geosynthetic layer for various soil reactions

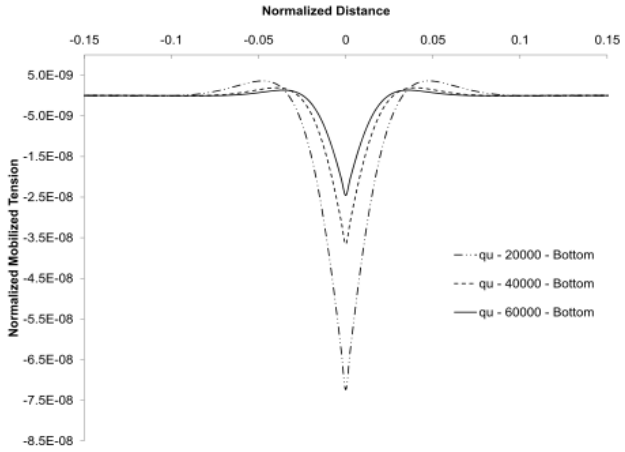


Fig. 17 Typical mobilized tension of bottom geosynthetic for various soil reactions

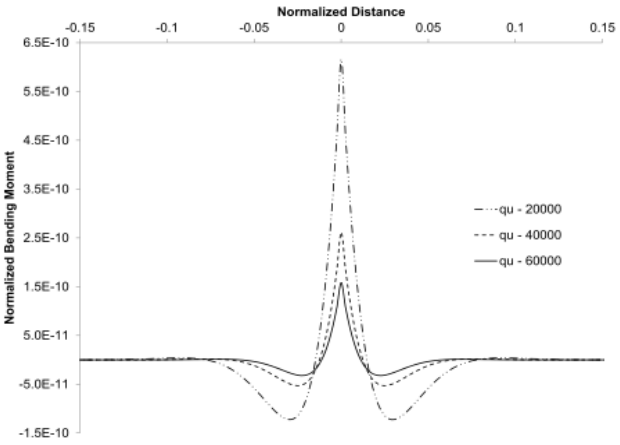


Fig. 18 Typical bending moment of beam for various soil reactions

Open Science Index, Geological and Environmental Engineering Vol:9, No:9, 2015 publications.waset.org/10002172/pdf

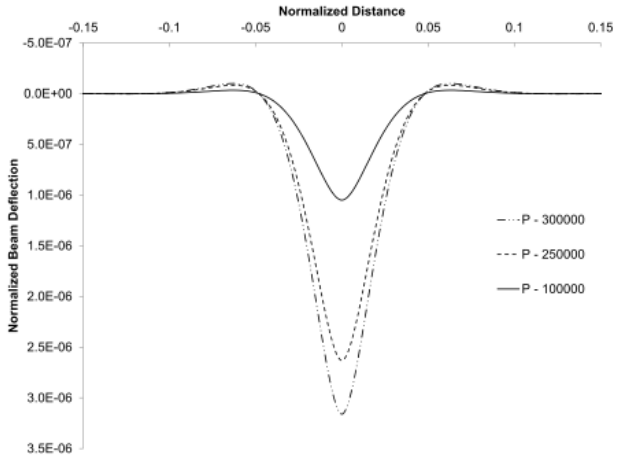


Fig. 19 Typical soil reaction variations for various load intensity

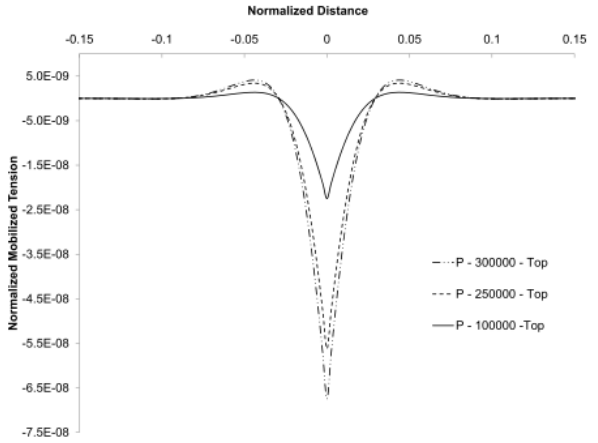


Fig. 20 Typical mobilized tension of top geosynthetic layer for various velocity values

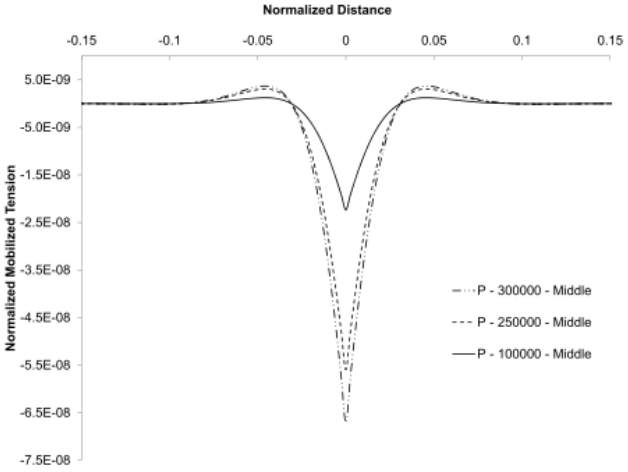


Fig. 21 Typical mobilized tension of middle geosynthetic layer for various velocity values

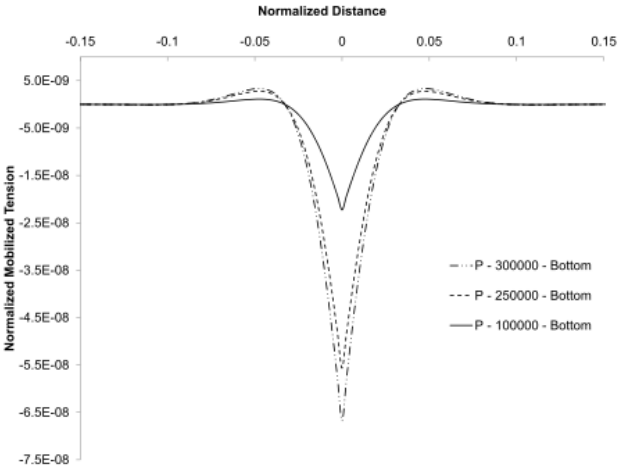


Fig. 22 Typical mobilized tension of bottom geosynthetic layer for various velocity values

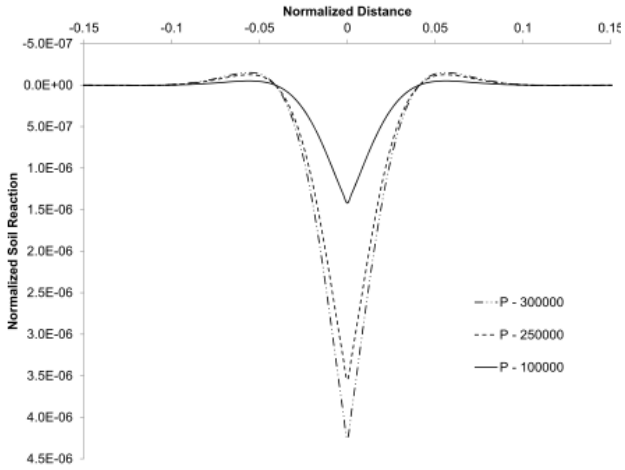


Fig. 23 Typical soil reaction variations for various load intensity

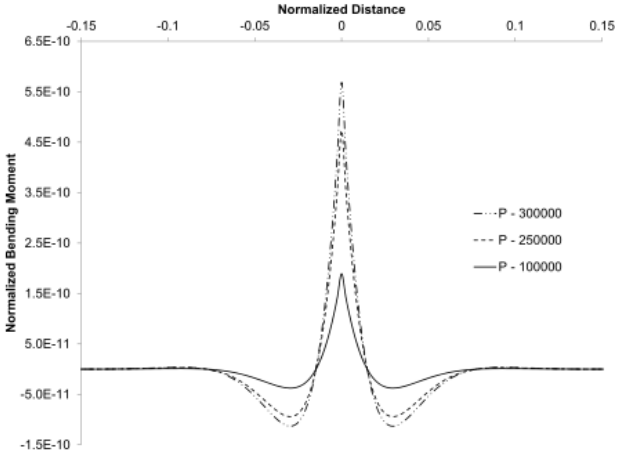


Fig. 24 Typical bending moment of beam for various soil reactions

The influence of ultimate resistance of poor foundation soil for multilayer extensible geosynthetic reinforced on response of soil- foundation system for the effect of magnitude of applied load has been depicted in Figs. 19-24 for the parameters, i.e. $G_{to}^{*}= G_{bo}^{*}=3x10^{-7}$, $I^{*}=6x10^{-10}$, $\tau_{ut}^{*}=\tau_{ub}^{*}=$

Open Science Index, Geological and Environmental Engineering Vol:9, No:9, 2015 publications.waset.org/10002172/pdf

$2.7x10^{-9}$,μ_t= μ_b=0.5, K=0.172, $q_u^*=1.8x10^{-5}$ and $\rho^*=1.2x10^{-7}$. The normalized magnitude of applied load has been varied from $3.0x10^{-7}$ to $7.5x10^{-7}$ and corresponding reduction in the maximum deflection of beam has been found to be 67 % (Fig. 19). It can be seen that deflection of the ground surface becomes zero when the deflection of the beam is negative, i.e, when beam is lifted up; there is a separation between the beam and the ground surface. The corresponding reduction in maximum normalized bending moment in the beam has been found to be 66 % (Fig. 24). Any increase in magnitude of load intensity causes more deflection and hence more bending moment. The influence of applied load on the tension mobilized in multilayer tensionless geosynthetic layer has been depicted in Figs. 20-22. The maximum mobilized tension occurs at the point of application of load and reduces on either side. This has been found to reduce by 66.7 % as the applied load reduces from $6.75x10^{-8}$ to $2.23x10^{-8}$. Soil reaction has been shown in Fig. 23 for different values of applied load as considered and the reduction in maximum soil reaction has been found to be about 66.7% for the reduction in applied load from $4.26x10^{-6}$ to $1.421x10^{-6}$.

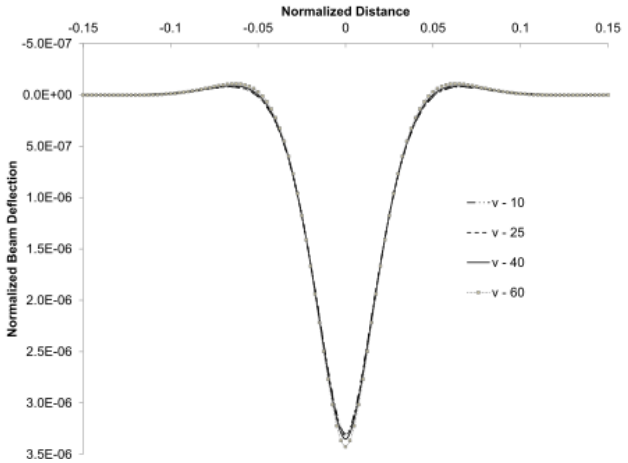


Fig. 25 Typical settlement profiles for various velocity values

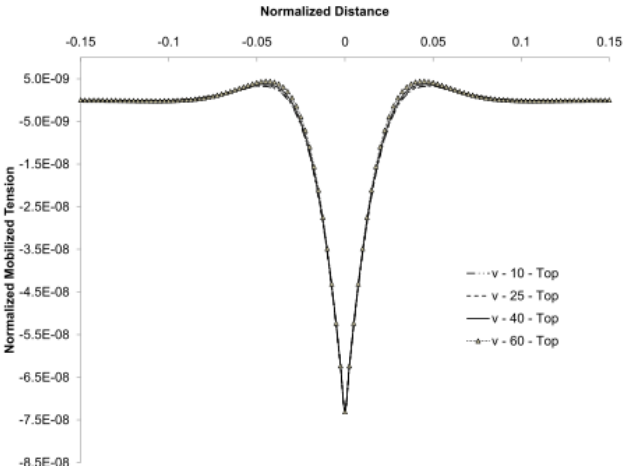


Fig. 26 Typical mobilized tension of top geosynthetic layer for various velocity values

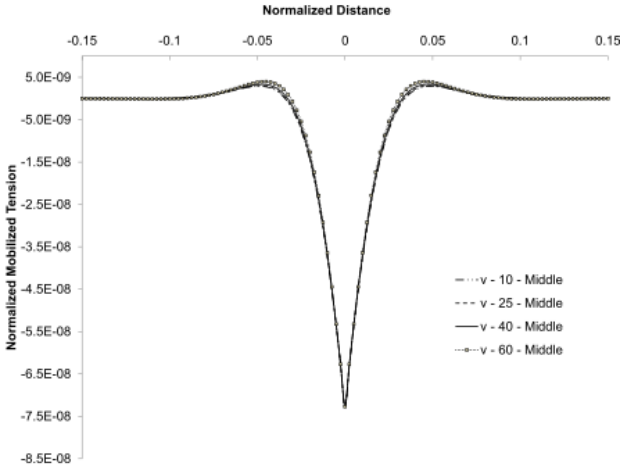


Fig. 27 Typical mobilized tension of top geosynthetic layer for various velocity values

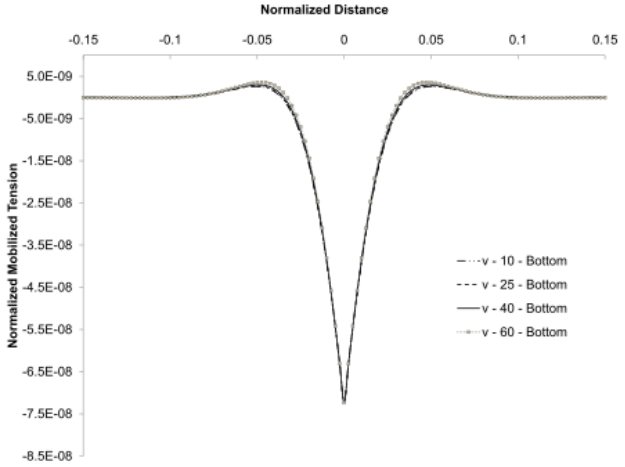


Fig. 28 Typical mobilized tension of middle geosynthetic layer for various velocity values

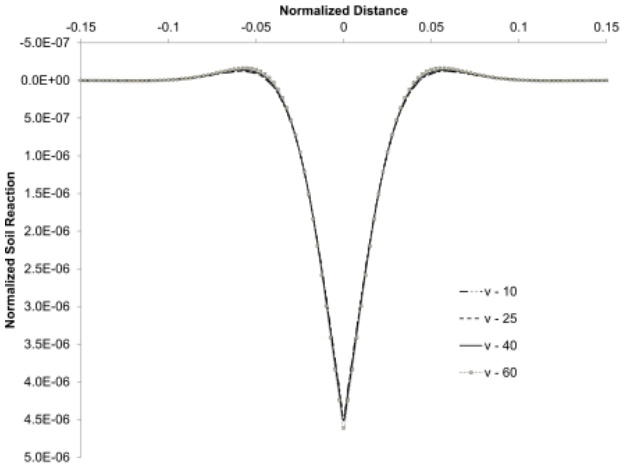


Fig. 29 Typical soil reaction profile for various velocity values

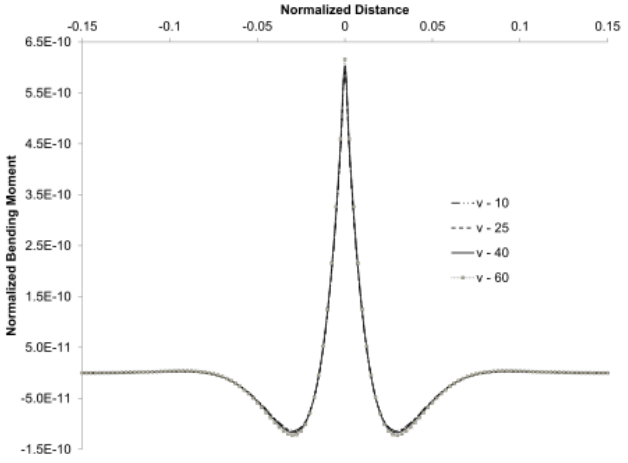


Fig. 30 Typical bending moment of beam for various velocity values

Effect of velocity of applied load, for multilayer extensible geosynthetic reinforced on response of soil-foundation system has been depicted in Figs. 25-29. For parameters, i.e., $P^*= 5.42x10^{-5}$; $G_{to}^*=G_{4o}^*= 1.63x10^{-5}$; K= 0.172; $I^*= 3.31x10^{-8}$, $\tau_{u1}^*=\tau_{u4}^*=1.5x10^{-4}$; $\mu_1=\mu_4= 0.5$ and $q_u^*=5.0x\ 10^{-4}$ on the deflection profile of infinite beam has been studied for the parameter velocity varying from 10 to 60. The maximum deflection has been found to reduce by about 3% as the velocity ranging from 3.43 x 10^{-6} to 3.3 x 10^{-6}. Figs. 25-28 show the effect of velocity of applied load on normalized mobilized tension in multilayer tensionless extensible geosynthetic layers. As expected, the mobilized tension in multilayer tensionless extensible geosynthetic layers has been found to reduce with an increase in the velocity of applied load. A reduction of about 10% in tension mobilized in multilayer extensible geosynthetic layers have been observed corresponding to an increase in velocity varying from 7.31x 10^{-8} to 7.22x 10^{-8}. Figs. 29 and 30 depict the soil reaction and bending moment respectively for various velocity of applied load. Although there is same influence of velocity of applied load on the response of soil - foundation system, however this has not been found to be significant.

VII. Conclusions

The proposed model analysis an infinite beam resting on multilayer tensionless extensible geosynthetic reinforced granular fill poor soil system under a concentrated load moving with constant velocity is presented. The analysis takes into account multilayer tensionless extensible geosynthetic and the nonlinear behavior of granular fill and the natural occurring poor soil. Thus, the separation of the beam from the ground surface has been incorporated in the present approach.

Based on the results and discussion presented in the previous section, the following generalized conclusions as given follows:

1. The lift up of the beam (negative deflection) and the mobilized tension in the multilayer tensionless geosynthetic layer are observed to be uniformly reduction as compared to the foundation reacting on compression as well as tension.
2. The response of the soil-foundation under consideration is greatly affected by the inclusion of nonlinearity in granular fill and the poor soil.
3. It is observed that the deflection, bending moment in the beam, mobilized tension and the soil reaction increases with the load intensity and in proportion to the increase in the applied load.
4. As the parameter velocity of applied load varies from $3.43x10^{-6}$ to $3.3x10^{-6}$, the maximum normalized deflection of the beam can reduce by about 3 % for the range of parameters considered in the study.
5. The ultimate resistance of poor soil has been found significantly affect the response of infinite beam and the geosynthetic layer. Deflection (about 56%) and bending moment in the beam (about 77%) has been found to reduce with an increase in the ultimate resistance of poor soil. Tension mobilized in the geosynthetic layer has been found to reduce by extent 67.3% for an increase in parameter qu from $2.0x10^4$ to $6.0x10^4$.

References

[1] Alekseyeva.L.A. (2006), "The Dynamic of an Elastic Half Space Under the Action of a Moving Load", Journal of Applied Mathematics and Mechanics, vol 71, pp. 511-518.
[2] Basu, D. (2001), "Soil Structure Interaction Analysis due to Moving Load". M.Tech. Thesis, Department of Civil Engineering, Indian Institute of Technology, Kanpur, India.
[3] Chandan Ghosh and Madhav M. R. (1994), "Settlement Response of a Reinforced Shallow Earth Bed", Geotext. Geomembranes, Vol. 13, pp.643– 656.
[4] Choros, J. and Adams, G. G. (1979). "A Steadily Moving Load on an Elastic Beam Resting on a Tensionless Winkler Foundation". Journal of Applied Mechanics Division, ASME, Vol. 46, No. 1, pp. 175-180.
[5] Duffy, D.G. (1990), "The Response of an Infinite Railroad Track to a Moving, Vibrating Mass", Journal of Applied Mechanics Division, ASME, Vol. 57, No. 1, pp. 66-73.
[6] Jaiswal, O.R. and Iyenger, R.N. (1997), "Dynamic Response of Railway Tracks to Oscillatory Moving Masses", Journal of Engineering Mechanics Division, ASCE, Vol. 123 No. 7, pp. 753-757.
[7] Karuppasamy, K (2010), "Non-Linear Response of Infinite Beams on Reinforced Earth Beds under Moving Load". M.Tech. Thesis, Department of Civil Engineering, Indian Institute of Technology, Roorkee, India.
[8] Kerr A.D (1964), "Elastic and Visco-Elastic Foundation Models", Journal of Applied Mechanics Division, Trans. of ASME 1964; 31 (3): 491-498.
[9] Kondner, R.L. and J.S. Zelasko. (1963), "A Hyperbolic Stress-Strain Response: Cohesive Soil", Journal of the Soil Mechanics and Foundations Division, ASCE, 89(SM1):115-143
[10] Lin, L., and Adams, G.G., (1987), "Beam on Tensionless Elastic Foundation Subjected to Moving Load", Vol. 113, No. 4.
[11] Sun Lu (2001). "Dynamic Displacement Response of Beam Type Structures to Moving Line Loads". International Journal of solids and structures, vol 38, pp 8869 - 8878.
[12] Maheshwari, P., Basudhar, P. K., and Chandra, S. (2004b) "Response of Beams on a Tensionless Extensible Geosynthetic-Reinforced Earth Bed Subjected to Moving Loads". Computer and Geotechnics, Vol. 31, pp. 537 – 548.
[13] Rao N.S.V. Kameswara (1974), "Onset of Separation between a Beam and Tensionless Foundation due to Moving Loads", Journal of Applied Mechanics Division, Trans. of ASME 41 (1): 303-305.
[14] Saito, H. and Teresawa, T. (1980), "Steady-State Vibrations of a Beam on a Pasternak Foundation for Moving Loads", Journal of Applied Mechanics Division, Trans. of ASME, Vol. 47, pp. 879-883.
[15] Selvadurai APS (1979), "Elastic Analysis of Soil–Foundation Interaction". Elsevier Scientific Publication Company, Amsterdam, The Netherlands, 543 pp.

Open Science Index, Geological and Environmental Engineering Vol:9, No:9, 2015 publications.waset.org/10002172/pdf

[16] Wang. M.C., Badie. A. and Davids. N. (1984), "Traveling Waves in Beam on Elastic Foundation", Journal of Engineering Mechanics Division, ASCE, Vol. 110, No. 6, pp. 879-893.
[17] Yin J. H. "Modeling of Geosynthetic-Reinforced Granular Fill over Soft Soil". Geosynthetic International 1997; 4(2): 165-85.
[18] Yin JH. "A Nonlinear Model of Geosynthetic-Reinforced Granular Fill over Soft Soil", Geosynthetic International 1997; 4(5): 523-37.
[19] Yin JH, "Closed Form Solution for Reinforced Timoshenko Beam on Elastic Foundation", J Appl Mech Div Trans, Am Soc. MechEng 2000; 12(8): 868-74.
[20] Islam, M. R., Rahman, M. T. and Tarefder, R. A. (2012). "Laboratory Investigation of the Stiffness and the Fatigue Life of Glass Grid Reinforced Asphalt Concrete." International Journal of Pavements, Vol. 11, No. 1, pp. 82-91.

Open Science Index, Geological and Environmental Engineering Vol:9, No:9, 2015 publications.waset.org/10002172/pdf